Int. J. Dev. Biol. 54: 655-665 (2010)
doi: 10.1387/ijdb.082845gd

THE INTERNATIONAL JOURNAL OF DEVELOPMENTAL BIOLOGY
www.intjdevbiol.com

Oscillatory Ca^{2+} dynamics and cell cycle resumption at fertilization in mammals: a modelling approach

GENEVIÈVE DUPONT*,[1], ELKE HEYTENS[2] and LUC LEYBAERT[3]

[1]*Unité de Chronobiologie Théorique, Université Libre de Bruxelles, Brussels,*
[2]*Department of Reproductive Medicine, Ghent University Hospital, Ghent and*
[3]*Department of Basic Medical Sciences, Physiology Group, Ghent University, Ghent, Belgium*

ABSTRACT Fertilization in mammals is accompanied by Ca^{2+} oscillations in the egg cytoplasm, leading to exit from meiosis and entry into the first embryonic cell cycle. The signal transduction pathway linking these Ca^{2+} changes to cell-cycle related kinases has not yet been fully elucidated, but involves activation of calmodulin-dependent kinase II (CaMKII). Here, we develop a computational model to investigate the mechanism by which cell cycle resumption can be sensitive to the temporal pattern of Ca^{2+} increases. Using a model for CaMKII activation that reproduces the frequency sensitivity of this kinase, simulations confirm that Ca^{2+} spikes are accompanied by in phase variations in the level of CaMKII activity and suggest that in most mammalian species, Ca^{2+} spikes are well suited to maximize CaMKII activation. The full model assumes that CaMKII brings about a decrease in the level of cyclinB-cdk1 by two pathways, only one of which is CSF-dependent. Parameters are selected to account for the experimental observations where mouse eggs were artificially activated by different Ca^{2+} stimulatory protocols. The model is then used in the context of 'assisted oocyte activation (AOA)' to investigate why the best rates of successful activation are obtained when eggs are submitted to two applications of Ca^{2+} ionophores.

KEY WORDS: *CaMKII, in vitro fertilization, calcium ionophore, assisted oocyte activation (AOA)*

Introduction

Fertilization is one of the most fundamental and fascinating phenomena in cell biology. In mammals, egg activation is governed by the interplay between two major cellular oscillators: Ca^{2+} oscillations and the cell cycle (Runft *et al.*, 2002; Jones, 2005). In these species indeed, sperm-egg fusion is associated with the delivery into the egg of a sperm specific phospholipase C, PLCζ which catalyses the synthesis of inositol-1,4,5-trisphosphate ($InsP_3$), a direct mediator of Ca^{2+} release from the endoplasmic reticulum (ER) (Saunders *et al.*, 2002). Thus, gamete fusion is rapidly followed by a massive Ca^{2+} rise in the cytoplasm, which propagates from the point of sperm attachment throughout the entire egg. This 'fertilization wave' is necessary to prevent polyspermy. It is followed by repetitive Ca^{2+} waves of lower amplitude and duration, which are required for completion of the meiotic cell cycle and for embryo development (Ozil, 1998). The period of these oscillations ranges from a few minutes to about half an hour, depending mainly on the species considered. They last 3-4 hours and cease around the time of pronuclear formation (Stricker, 1999).

As in somatic cells, Ca^{2+} oscillations in fertilized eggs rely on the dynamical properties of the $InsP_3$ receptor. This receptor/Ca^{2+} channel located in the membrane of the ER is regulated by Ca^{2+} in a biphasic manner: low concentrations of Ca^{2+} in the cytosol activate Ca^{2+} release (a process known as CICR for 'Ca^{2+}-induced Ca^{2+} release'), while higher levels of this ion inhibit further liberation from the ER. Such type of regulation is well-known to give rise to sustained oscillations. The detailed mechanism of regulation of this receptor has been extensively characterized, both from an experimental and modelling point of view (Sneyd *et al.*, 1995; Berridge, 2008; Dupont *et al.*, 2007). However, Ca^{2+}-dependent $InsP_3$ production also plays a role at fertilization as PLCζ is Ca^{2+}-sensitive (Saunders *et al.*, 2002; Swann and Yu, 2008), a phenomenon that may be responsible for the specific shape of the fertilization Ca^{2+} wave (Fall *et al.*, 2004; Dupont and

Abbreviations used in this paper: AOA, assisted oocyte activation; CaMKII, calmodulin-dependent kinase II.

***Address correspondence to:** Geneviève Dupont. Université Libre de Bruxelles, Campus Plaine CP231, Boulevard du Triomphe, B-1050 Brussels, Belgium. Fax:+32-2-650 57 67. e-mail: gdupont@ulb.ac.be - web: http://www.ulb.ac.be/sciences/utc

Accepted: 11 May 2009. *Final author-corrected PDF published online:* 12 January 2010.

ISSN: Online 1696-3547, Print 0214-6282

Dumollard, 2004).

The cell cycle machinery has also been widely investigated. It is since long known that the periodicity of the cell cycle relies on a biochemical oscillator in which a complex made of cyclin B1 and cdc2 kinase (also known as cdk1) plays a central role. The activity of this complex, called MPF for 'maturation promoting factor', peaks at each cell division. However, all transitions between the various phases of the cell cycle (G1-S-G2-M) are governed by cyclin-cdk complexes, which are themselves submitted to extensive regulation by an intricate network of signalling molecules (Nurse, 2002). A unique and particularly interesting case of control is that of meiosis in mammals. In these species indeed, ovulation occurs when oocytes are fully grown and put in an arrested state corresponding to the metaphase of the second meiotic division. This arrest is characterized by a high and constant level of MPF and by the presence of a metaphase spindle. It is relieved by the transient Ca^{2+} increase occurring at fertilization. The activity responsible for this arrest is still in the process of being elucidated and is referred to as cytostatic factor (CSF; Masui and Market, 1971). CSF activity results in the inhibition of the anaphase-promoting complex cyclosome (APC), an E3 ubiquitin ligase complex that molecularly earmarks securin –a protein that maintains sister chromatin cohesion– and cyclin B1 for destruction. Thus, as cyclin B1 cannot be degraded anymore, MPF accumulates and no cyclic variation of this compound corresponding to the progression in the cell cycle can occur (see Madgwick and Jones, 2007 for review).

The mechanism of CSF arrest has been best characterized in the frog, where it includes a pathway involving the proto-oncogene Mos and a mitogen-activated protein kinase (MAPK; Sagata *et al.*, 1989), but the primary role of this pathway in mammals is less clear (Jones, 2005). Moreover, another specific APC inhibitor, the early mitotic inhibitor Emi2, has been shown to be involved in both the establishment and maintenance of metaphase II arrest in frog and mice (Schmidt *et al.*, 2005). At fertilization, Ca^{2+}-activated CaMKII phosphorylates Emi-2, creating a docking site for the Polo-like kinase Plx1, which, in turn generates a second phosphorylation in Emi-2. This second site earmarks Emi2 for degradation, thus relieving APC inhibition (Rauh *et al.*, 2005; Hansen *et al.*, 2006; Madgwick *et al.*, 2006). Interestingly, it has been proposed recently that CSF could imply both the Emi2 and the c-Mos/MAPK pathway (Madgwick *et al.*, 2007).

CaMKII plays a key role at fertilization, as in many other vital physiological processes (Braun *et al.*, 1995). Expression of a constitutively active form of CaMKII indeed promotes destruction of cyclin B1 and securin, and results in the completion of meiosis (Madgwick *et al.*, 2005; Knott *et al.*, 2006). In physiological situations, CaMKII activity has been shown to oscillate in synchrony with fertilization-induced Ca^{2+} oscillations (Markoulaki *et al.*, 2004). The possible implications of an oscillatory Ca^{2+} signal on cell cycle resumption in mammals have been extensively investigated. These studies have demonstrated that the temporal pattern of Ca^{2+} changes (amplitude, duration and frequency) has specific effects not only on the immediate events of egg activation, but also on long-range events in the pre-implantation period (for reviews, see Ducibella *et al.*, 2006; Malcuit *et al.*, 2006; Ducibella and Fissore, 2008). In contrast to other Ca^{2+}-activated processes where the cellular response is specifically related to the frequency or waveform of Ca^{2+} oscillations (Larsen *et al.*, 2004; De Pitta *et al.*, 2008; see Dupont *et al.*, 2007 for review), egg activation seems to be regulated by the summation of Ca^{2+} increases. Thus, very distinct Ca^{2+} signals can lead to cell cycle resumption and an optimization of these stimulatory protocols may have important implications in veterinary, medical and cloning contexts.

In the present study, we use a computational model to investigate in a systematic way the link between Ca^{2+} increases and egg activation in mammals. CaMKII activation is described by a set of equations that have been shown to quantitatively reproduce the frequency sensitivity of this kinase (Dupont *et al.*, 2003). We thus analyse how fertilization-induced Ca^{2+} changes modulate CaMKII activity and find that the characteristics of these oscillations are well suited to maximize CaMKII activation. To describe the interaction between CaMKII and the signalling molecules driving the early embryonic cell cycle, we have adapted and updated a model published 10 years ago (Dupont, 1998). A set of 3 ordinary differential equations describes the evolution of cyclin B1 concentration, MPF activity and activity of the APC complex (Goldbeter, 1991). This core model for the cell cycle can switch from an oscillatory behaviour to an arrested state when APC activation is prevented, corresponding to the CSF-induced metaphase II arrest. In the model, CaMKII is assumed to have a dual effect on egg activation: on one hand, it activates a signalling pathway leading to CSF degradation, and, on the other hand, it activates APC in a fast and transient manner. The existence of the latter pathway is required to account for the possibility of a metaphase III (MIII) arrest, a pathological state of the egg that results from an insufficient activation by Ca^{2+} (Kubiak *et al.*, 1992). The model can also account for the experimental results of Toth *et al.* (2006), where mouse eggs were artificially activated by different Ca^{2+} stimulatory protocols of different frequencies, durations and amplitudes. We then used the model in the context of 'assisted oocyte activation (AOA)' and discuss the molecular mechanism underlying the observation that the best rates of successful activation are obtained when eggs are submitted to two applications of Ca^{2+} ionophores (Heytens *et al.*, 2008a).

Model description

Model for CaMKII activation

CaMKII is composed of 10-12 subunits, arranged in a 'hub-and-spoke' structure (Morris and Török, 2001). Each subunit possesses a regulatory and a catalytic site. In low Ca^{2+}, the catalytic site is covered by an inhibitory segment. Upon Ca^{2+}-CaM binding, a conformational change relieves the kinase subunit from the auto-inhibition mechanism. This subunit then becomes active and can thus phosphorylate exogenous substrates as well as Ca^{2+}-CaM bound neighboring subunits of the same holoenzyme (Mukherji & Soderling, 1994). This inter-subunit phosphorylation disrupts the interaction between the auto-inhibitory domain and the catalytic site. Thus, an autophosphorylated subunit remains active, even after dissociation of Ca^{2+}-CaM. Autophosphorylation also increases the affinity of CaM to the subunit, leading to the concept of CaM trapping.

Based on this regulatory pathway, we have previously developed a simple computational model accounting for the frequency sensitivity of CaMKII observed *in vitro* by De Koninck and Schulman (1998). The model (Fig. 1) is based on the description of the time evolution of the subunits in the different states, regardless of their

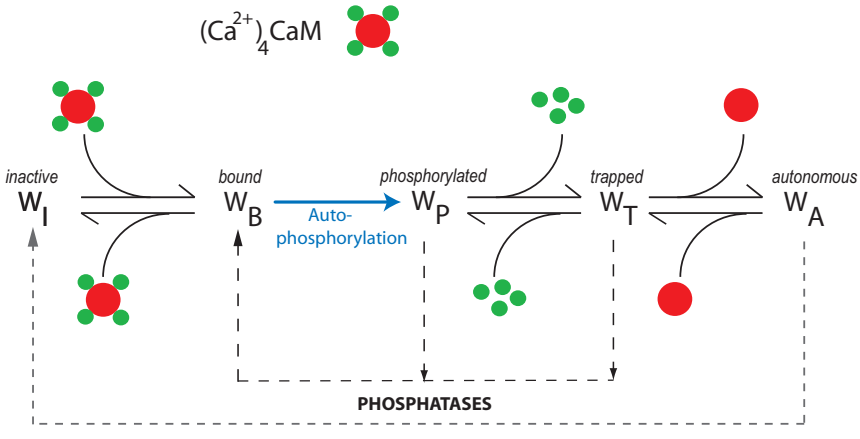

Fig. 1. Schematic representation of the model used to simulate the dynamics of CaMKII activation by Ca^{2+}-CaM. *The W_i's represent the specific states of the kinase subunits. Except for W_I that is inactive, all these states are characterized by some specific level of activity. This model is similar to that of Dupont* et al. *(2003), except that it considers the presence of phosphatases in the egg cytoplasm, which are represented by the dashed arrows. The arrow linking W_T to W_B through dephosphorylation also includes Ca^{2+} binding on the subunit-bound CaM.*

association to a specific holoenzyme. The variables of the models are thus the fractions of subunits in the inactive (W_I), Ca^{2+}-CaM bound (W_B), autophosphorylated (W_P), trapped (W_T) and autonomous (W_A) states. Each state of the subunits is characterized by an 'activity coefficient' (c_i) that measures its phosphorylation activity compared to the maximum Ca^{2+}-CaM-stimulated activity, which occurs for the subunits in the bound, phosphorylated state (W_P). The complex that binds W_I is made of one CaM molecule and 4 Ca^{2+} ions. A quasi-equilibrium assumption is made on the reaction of Ca^{2+} binding to CaM. The transitions between the various possible states of the kinase are described by classical kinetic terms (see Dupont *et al.*, 2003 for a full description of the equations). Thus, for example, the evolution equation for the fraction of subunits in the Ca^{2+}-CaM-bound unphosphorylated state (W_B) is given by

$$\frac{dW_B}{dt} = k_{IB}\left[Ca^{2+} - CaM\right]W_I - k_{BI}W_B - V_A \qquad (1)$$

where V_A stands for the autophosphorylation rate.

Autophosphorylation is the only step that cannot be modelled by a simple, mass action kinetic expression. W_B can indeed only be phosphorylated by an *adjacent*, active subunit. As we do not consider the spatial arrangement of the subunits in the holoenzyme, we incorporate in this rate expression a function that takes into account the probability of an active subunit to be adjacent to another active subunit. Thus,

$$V_A = K_A\Big((c_B W_B)^2 + (c_B W_B)(c_P W_P) + (c_B W_B)(c_T W_T) + (c_B W_B)(c_A W_A)\Big) \qquad (2)$$

with $K_A = K'_A\left\{aT + bT^2 + cT^3\right\}$ where $T = W_B + W_P + W_T + W_A$.

The parameters defining this empirical function, which is a cubic function of the total fraction of active subunits, have been fitted to get quantitative agreement with experimental data.

The model was initially built to simulate the *in vitro* experiments performed by De Koninck and Schulman (1998), where CaMKII was immobilized in a PVC tubing and subjected to pulses of Ca^{2+}-CaM of variable duration, amplitude and frequency and in which no phosphatase was present. To represent a realistic egg cytoplasm, as well as to account for the observed decrease of CaMKII activity after each fertilization-induced Ca^{2+} spike (Markoulaki *et al.*, 2004), phosphatases were taken into account in the model (dashed lines in Fig. 1). Parameters characterizing phosphatases activity are listed in Table 1, together with those characterizing the CaMKII subunit kinetics which are the same as in (Dupont *et al.*, 2003) but are listed for convenience. For simplicity, Ca^{2+} increases are modelled as square wave pulses, allowing for a direct control of their amplitude, duration and frequency.

Minimal model for the early embryonic cell cycle

The set of biochemical reactions associated with cell cycle progression and control is a very active topic of investigation (Nurse, 2002). Many of these processes have been modelled in detail (Csikasz-Nagy *et al.*, 2006). Here, we focus on the early embryonic cell cycle, and more specifically on the events leading to the decrease in MPF after meiosis II arrest. Thus, we use a very simple, 3 variable model that incorporates the essential features of the cell cycle dynamics (Goldbeter, 1991). This model has already been used to investigate the link between cell cycle resumption and Ca^{2+} dynamics (Dupont, 1998). In the present work, we take into account new experimental findings. Thus, on

TABLE 1

PARAMETERS OF THE MODEL FOR CAMKII ACTIVATION SCHEMATIZED IN FIG. 1

k_{IB}	Rate of association of Ca^{2+}-CaM to a non-phosphorylated subunit	0.60 $nM^{-1}min^{-1}$
k_{BI}	Rate of dissociation of Ca^{2+}-CaM from a non-phosphorylated subunit	48 min^{-1}
k_{PT}	Rate of dissociation of Ca^{2+} from CaM bound to a phosphorylated subunit	60 μM^{-4} min^{-1}
k_{TP}	Rate of association of Ca^{2+} to CaM bound to a phosphorylated subunit	60 min^{-1}
k_{TA}	Rate of dissociation of CaM from a phosphorylated subunit	$k_{BI}/1000$
k_{AT}	Rate of association of CaM to a phosphorylated subunit	k_{IB}
K'_A	Phenomenological rate constant for autophosphorylation	17.4 min^{-1}
a	Factor in the empirical function for autophosphorylation, equ. (2)	-0.220
b	Factor in the empirical function for autophosphorylation, equ. (2)	1.826
c	Factor in the empirical function for autophosphorylation, equ. (2)	-0.800
V_{MP}	Normalized maximal rate of dephosphorylation	5 10^{-3} min^{-1}
K_P	Normalized Michaelis-Menten constant for phosphatases	0.3
c_I	Kinase activity of the W_I state	0
c_B	Kinase activity of the W_B state	0.75
c_P	Kinase activity of the W_P state	1
c_T	Kinase activity of the W_T state	0.8
c_A	Kinase activity of the W_A state	0.8
CaM_T	Total calmodulin concentration	1 μM

These parameters have been shown to reproduce the frequency sensitivity of CaMKII demonstrated by De Koninck and Schulman (1998). Here, phosphatases are also taken into account. Concentrations of CaMKII subunits are normalized with respect to the total concentration of enzyme subunits, which must not be considered explicitly. Parameter values correspond to the α isoform of CaMKII, which has been shown to be active in the egg cytoplasm (Madgwick *et al.*, 2005).

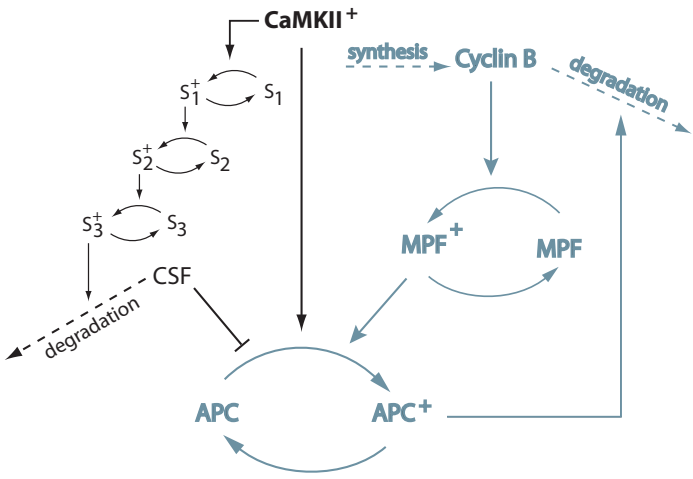

Fig. 2. Schematic representation of the model linking CaMKII activation and cell cycle resumption. *The superscript + always refers to an activated state. Indicated in grey is the part of the model corresponding to the minimal model for the cell cycle (Goldbeter, 1991). Before fertilization, the cell cycle is in an arrested state because of the inhibitory effect of CSF on APC activation. Erp1/Emi2 appears as a major component of this arresting factor (Schmidt* et al.*, 2006). CaMKII activation (resulting from a Ca^{2+} increase) triggers a signalling pathway that leads to CSF degradation. To take into account the existence of some time delay between CaMKII activation and CSF degradation, this pathway involves 3 hypothetical mediator proteins S_1, S_2 and S_3. We also assume that CaMKII+ can directly activate APC, through a faster, but still unidentified, mechanism.*

one hand we introduce a realistic model for CaMKII activation (see section 1 just above) and, on the other hand, we incorporate adequate regulatory elements between Ca^{2+} increases and cell cycle progression.

Fig. 2 schematizes the model simulated in the present study. The components that are strictly associated with the cell cycle are indicated in grey. In this part, three variables are considered: the concentration of cyclin B, the fraction of active MPF (denoted by MPF^+) and the fraction of active proteolytic complex, APC (denoted by APC^+). The concentration of cyclin B varies because of synthesis and degradation. Cyclin B activates a phosphatase, called cdc25, which brings an inactive cdc2 kinase into an active, dephosphorylated state. For simplicity, the step accounting for the formation of this heterodimer is not explicitly considered in the model, and thus, the active MPF (M^+) is represented in the model as a fraction of the active form of cdc2 kinase. Phosphorylation (deactivation) of cdc2 is mediated by the wee1 kinase. Unphosphorylated cdc2 (M^+) triggers the activation of APC, which labels cyclins for degradation through the ubiquitin pathway. Inactivation of APC occurs through dephosphorylation by a phosphatase. The negative feedback exerted by APC on the level of cyclin is at the core of the oscillatory mechanism. The temporal evolution of the three variables of the model is thus given by the following differential equations (see Goldbeter, 1991 for a detailed presentation of the model):

$$\frac{dC}{dt} = v_i - V_d X^+ \frac{C}{K_d + C} - k_d C \qquad (3)$$

$$\frac{dM^+}{dt} = V_{M1} \frac{C}{K_c + C} \frac{1 - M^+}{K_1 + 1 - M^+} - V_2 \frac{M^+}{K_2 + M^+} \qquad (4)$$

$$\frac{dX^+}{dt} = V_3 M \frac{1 - X^+}{K_3 + 1 - X^+} - V_4 \frac{X^+}{K_4 + X^+} \qquad (5)$$

where C denotes the concentration of cyclin, while X^+ and M^+ stand for the fractions of active APC and MPF, respectively. A description of the parameters, together with their values used in the simulations, is given in Table 2.

Unfertilized mammalian eggs are arrested in the metaphase of the second meiosis, in a state characterized by a high level of cyclin and active MPF. This is due to the presence of a substance, known as cytostatic factor (CSF) in the egg cytoplasm. Erp1/Emi2 appears as a major component of this arresting factor (Schmidt *et al.*, 2006). It acts by preventing the activation of APC. CSF is known to be degraded following CaMKII activation, which allows for resumption of the cell cycle. As the molecular mechanism by which CaMKII governs CSF degradation still remains to be fully elucidated, we assume here that this process is brought about by a cascade of post-translational modifications, allowing for the existence of some delay between CaMKII activation and CSF degradation. Such delay is formalized in the model by the sequential activation of three unknown molecular effectors (S_1, S_2 and S_3 as shown in Fig. 2). In principle, this model with CaMKII-activation of CSF degradation could account on its own for the fact that a sufficient increase in cytosolic Ca^{2+} can resume the cell cycle. However, the existence of a CSF-independent pathway for MPF

TABLE 2

PARAMETERS OF THE MODEL FOR CELL CYCLE RESUMPTION SCHEMATIZED IN FIG. 2 AND DEFINED BY EQS. (3)-(8)

v_i	Rate of cyclin synthesis	5.7 10^{-4} μMmin^{-1}
V_d	Maximal rate of cyclin degradation	0.0343 μMmin^{-1}
K_d	Michaelis-Menten constant for cyclin degradation	0.005 μM
k_d	Rate constant for non-regulated cyclin degradation	2.29 10^{-4} min^{-1}
V_{M1}	Normalized maximal rate of MPF activation	0.0686 min^{-1}
K_1	Normalized Michaelis-Menten constant for MPF activation	5 10^{-3}
K_c	Half-saturation constant for cdc25 activation by cyclin	0.5 μM
V_2	Normalized maximal rate of MPF inactivation	0.0353 min^{-1}
K_2	Normalized Michaelis-Menten constant for MPF inactivation	5 10^{-3}
V_{M3}	Normalized maximal rate of APC activation	0.0178 min^{-1}
K_3	Normalized Michaelis-Menten constant for APC activation	5 10^{-3}
V_4	Normalized maximal rate of APC inactivation	0.00914 min^{-1}
K_4	Normalized Michaelis-Menten constant for APC inactivation	5 10^{-3}
V_{AM1}	Normalized maximal rate of S_1 activation	0.098 min^{-1}
V_{D1}	Normalized maximal rate of S_1 inactivation	3 10^{-3} min^{-1}
V_{AM2}	Normalized maximal rate of S_2 activation	13.3 min^{-1}
V_{D2}	Normalized maximal rate of S_2 inactivation	0.93 min^{-1}
V_{AM3}	Normalized maximal rate of S_3 activation	1.33 min^{-1}
V_{D3}	Normalized maximal rate of S_3 inactivation	0.93 min^{-1}
K_{A1}	Normalized Michaelis-Menten constant for S_1 activation	0.05
K_{D1}	Normalized Michaelis-Menten constant for S_1 inactivation	0.05
K_{A2}, K_{A3}	Normalized Michaelis-Menten constant for S_2, S_3 activation	0.01
K_{D2}, K_{D3}	Normalized Michaelis-Menten constant for S_2, S_3 inactivation	0.01
V_{M9}	Maximal rate for CSF degradation	0.10 μMmin^{-1}
K_9	Michaelis-Menten constant for CSF degradation	0.5 μM
k_9	Rate constant for non-regulated CSF degradation	6.7 10^{-5} min^{-1}
K_i	Half-saturation constant for inhibition of APC activation by CSF	0.5 μM
CSF_0	Initial concentration of CSF	1 μM

See text for the discussion about the choice of parameter values. Concentrations of active MPF, APC, S_1, S_2 and S_3 are expressed as fractions of the total concentrations of these proteins, respectively.

inactivation has been proposed earlier (Watanabe *et al.*, 1991). Such a pathway is indeed necessary to account for some experimental observations, as the possible arrest of mammalian eggs in metaphase III, a pathological state resulting from an incomplete activation of the egg (Kubiak *et al.,* 2008) or the fact that the decrease in MPF activity following one Ca^{2+} spike is only transient (Collas *et al.*, 1995). As there is no synthesis of CSF in metaphase-arrested eggs, a *transient* activation of APC can only be explained by the existence of another pathway. Thus, in the model, we assume a direct activation of APC by active CaMKII. The real pathway responsible for this activation remains to be identified, and may involve the mos/MAPK pathway. The only important assumption relevant to the behaviour of the model is that this pathway is much faster than the CamKII-induced stimulation of CSF degradation. The detailed form of the direct activation of APC by CaMKII has been modified with respect to the previous model (Dupont, 1998). In this version of the model indeed, the cell cycle could not resume as long as Ca^{2+} is still spiking, which does not happen *in vivo* (Ozil *et al.*, 2005). To get a full description of the model schematized in Fig. 2, one needs to consider the following equations:

$$\frac{dS_i}{dt} = V_{Di}\frac{1-S_i}{K_{Ai}+1-S_i} - V_{Ai}\frac{S_i}{K_{Di}+S_i} \quad \text{for i=1,2,3} \qquad (6)$$

with

$$V_{A1} = V_{AM1}\left(c_2.W_P + c_3.W_T + c_4.W_A\right)\ ;\ V_{A2} = V_{AM2}\left(1-S_1^4\right)$$

and $V_{A3} = V_{AM3}\left(1-S_2\right)$

$$\frac{dCSF}{dt} = -V_{M9}.(1-S_3).\frac{CSF}{K_9+CSF} - k_9.CSF \qquad (7)$$

In each case, S_i stands for the fraction of effector i in the inactive state. Thus, $S_i^+ = 1\text{-}S_i$ stands for the fraction of effector i in the active state. To account for the inhibition of APC activation by CSF and of its direct activation by CaMKII, V_3 appearing in equ. (5) is given by:

$$V_3 = V_{M3}.\left(M.\frac{K_i^4}{K_i^4+CSF^4} + c_2.W_P + c_3.W_T + c_4.W_A\right) \qquad (8)$$

Except for cyclin B (C) and CSF, all variables are defined as fractions of molecules in the active or inactive states. Meanings and values of the parameters appearing in these equations are given in Table 2.

Results

CaMKII responses to fertilization-induced Ca^{2+} changes

Fertilization is associated with a large Ca^{2+} increase that triggers the events of egg activation. CaMKII mediates most of these events as recruitment of maternal mRNAs and cell cycle resumption and participates to cortical granule exocytosis and block to polyspermy. *In vitro*, this enzyme has been shown to be sensitive to the temporal pattern of Ca^{2+} oscillations, and particularly to their frequency in the Hertz range (De Koninck and Schulman, 1998). We investigate, by means of a computational model that quantitatively reproduces this frequency sensitivity

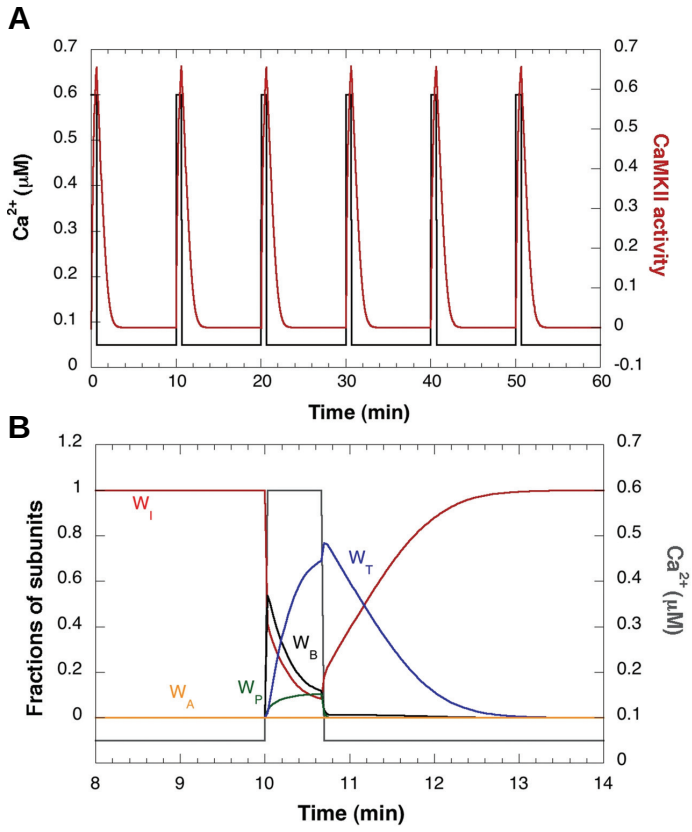

Fig. 3. Simulations of the variations of CaMKII activity in response to Ca^{2+} peaks reproducing fertilization-induced Ca^{2+} oscillations. (A) *Ca^{2+} spikes (in black) correspond to the square-wave pulses of Ca^{2+} increases from a basal level equal to 50 nM up to 600 nM, and lasting 40s. The period is fixed at 10 min. The kinetics of CaMKII activation (in red) closely follows the kinetics of the Ca^{2+} peaks.* **(B)** *Detailed evolution of the fractions of subunits in the various possible states of the kinase during one Ca^{2+} peak. Results have been obtained by numerical integration of the model schematized in Fig.1 with mass-action kinetics, except for autophosphorylation that is given by equ. (2). Parameter values are listed in Table 1. CamKII activity is defined as $c_B.W_B + c_P.W_P + c_T.W_T + c_A.W_A$.*

(see section 2.1), the pattern of CaMKII activation resulting from fertilization-induced Ca^{2+} spikes. Fig. 3A shows that, in the model, a single Ca^{2+} spike, mimicked by a square-shaped Ca^{2+} increase from 50 to 600 nM during 40s, leads to a significant activation of the kinase. As such a spike roughly corresponds to physiological conditions in most mammalian species, except for the first activation wave that is anyway much larger, the model suggests that the frequency sensitivity of the kinase cannot be operative at fertilization. Frequency sensitivity is indeed associated with a *progressive* accumulation of the active subunits of the kinase. This result is in agreement with experimental results of Markoulaki *et al.* (2004, 2007) showing that each Ca^{2+} peak induces a similar increase in the level of CaMKII activity. Moreover, due to the presence of phosphatases in the egg cytoplasm, this activity drops as Ca^{2+} goes back to the resting level between successive spikes, thus leading to oscillations of CaMKII activity that are in phase with Ca^{2+} oscillations (Markoulaki *et al.*, 2004). Incorporation of phosphatases in the model leads to the same temporal

pattern of CaMKII activation (Fig. 3A). In the absence of data about phosphatase activities in eggs, parameter values for phosphatases were chosen in order to get a decrease in activity to basal levels in 1-2 min, as observed in experiments.

During each Ca^{2+} spike, there is a considerable adjustment of the various states of the subunits of the kinase, as shown in Fig. 3B. This Figure shows the temporal evolution of the fraction of subunits of the kinase in their different states during the course of one Ca^{2+} spike, indicated in grey. At the resting level of Ca^{2+} (50 nM), all subunits are in the inactive state (red). Upon an increase in Ca^{2+}, about half of these bind the Ca^{2+}-CaM complex very rapidly. This corresponds to the increase in the fraction of subunits in the W_B state (see Fig. 1 and black curve in Fig. 3B). After about ten seconds, autophosphorylation occurs (increase in W_P, see green curve). However, once a subunit has become phosphorylated, it rapidly shifts into a state where the Ca^{2+}-CaM complex becomes trapped (blue curve corresponding to the dissociation of Ca^{2+} from the W_P state). Thus, W_P does not accumulate because it is very rapidly transformed into W_T. The abrupt decrease in Ca^{2+} then slightly displaces the W_P/W_T ratio towards lower values (small 'bump' in the blue curve). Finally, as total CaM remains constantly high, CaM does not dissociate and there is almost no transition to the autonomous state. Thus, the fraction of active subunits (the vast majority of which are in the W_T state) decreases because of dephosphorylation by phosphatases. States W_B, W_P, W_T and W_A all contribute with slightly different weights to the total CaMKII activity, shown in red in Fig. 3A.

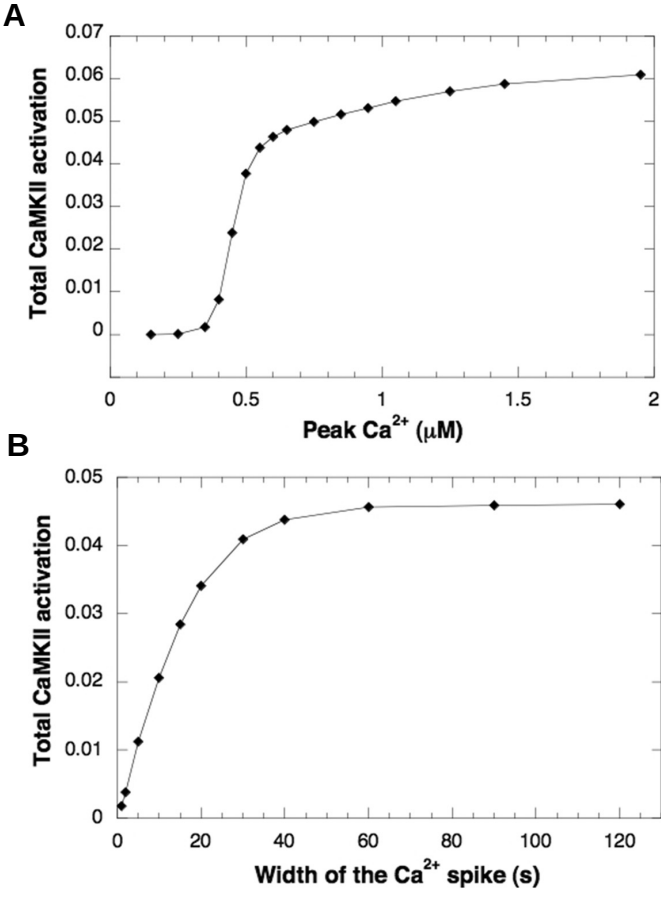

Fig. 4. Effect of the characteristics of the Ca^{2+} peaks on CaMKII activation. (A) *Total CaMKII activation (measured as the area of the peak of CaMKII activity) as a function of the amplitude of the Ca^{2+} peak.* **(B)** *Total CaMKII activation as a function of the duration of the square-wave Ca^{2+} increase. Results have been obtained with the same equations and parameter values as in Fig. 3.*

The question has been raised by a few authors if measuring the autonomous CaMKII activity after freezing the egg once the desired Ca^{2+} level had been reached was reliable to detect the total CaMKII activity, or if the kinase activity was underestimated in this type of assay (Markoulaki *et al.*, 2007; Ducibella & Fissore, 2008). Such an underestimation would be caused by the presence in the egg of subunits that have bound the Ca^{2+}/CaM complex and are thus active but are not yet phosphorylated (W_B state in the model). When transferred in a Ca^{2+} and CaM free medium, these subunits indeed rapidly switch into the inactive state (W_I in the model). In contrast, all phosphorylated subunits (W_P and W_T) would switch to the autonomous state as the medium for the assay does not contain phosphatases. Simulations shown in Fig. 3B indicate that some underestimation might indeed occur in these experiments when the egg is frozen during the Ca^{2+} peak. In particular, at the beginning of the Ca^{2+} spike, this underestimation can be of the order of the measurement itself (see the black curve as compared to the sum of the green, blue and yellow ones).

The influence of the amplitudes and widths of the Ca^{2+} spikes occurring at fertilization on the level of CaMKII activation can easily be analyzed with the model. In Fig. 4, we have computed the total CaMKII activity, as defined by the integral of one peak of CaMKII activity, for different amplitudes and widths of Ca^{2+} increases. It is clear from Fig. 4A that there is some threshold in the amplitudes of the Ca^{2+} spikes leading to CaMKII activation. Thus, if the Ca^{2+} spikes do not reach ~ 500 nM, the level of activation of CaMKII is not significant. At about 600 nM Ca^{2+}, CaMKII activation is nearly maximal and after this value, a further increase in the Ca^{2+} spike amplitude only slightly increases the CaMKII response. Spike duration also affects the extent of kinase activation. As shown in Fig. 4B, activation increases roughly linearly with the duration of the Ca^{2+} peak up to ~30s and then rapidly reaches the plateau. All together, the results shown in Fig. 4 suggest that in most mammalian species, the amplitude and duration of the sperm-induced Ca^{2+} spikes are well suited to maximize CaMKII activation.

CaMKII-mediated cell cycle resumption

As the amplitudes and durations of the fertilization-induced Ca^{2+} spikes do not result into a progressive activation of CaMKII, the requirement for long-lasting activation by Ca^{2+} for cell cycle resumption must originate from the interplay between CaMKII and the cell cycle-associated proteins. The model proposed for this interplay is schematized in Fig. 2 and explained in section 2.2. Fig. 5 shows the behaviour of this full model when the egg is submitted to 13 Ca^{2+} spikes with a period of 15 min, an amplitude of 800 nM and a duration of 40 s. Lasting thus for 3 hours (indicated by the grey region in Fig. 5), this protocol approximates Ca^{2+} oscillations seen at fertilization in mouse eggs. The inset shows the evolution of cytosolic Ca^{2+} and cyclin B concentrations in the course of time for the first 200 min after fertilization. Even at high levels of CSF, cyclin B decreases in response to Ca^{2+} spikes, due to the fast APC activation by CaMKII. This decrease

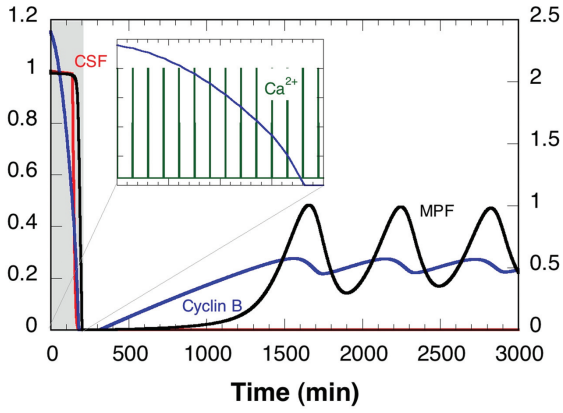

Fig. 5. Resumption of the cell cycle in response to fertilization-like Ca^{2+} oscillations. *The grey-shaded region corresponds to 19 Ca^{2+} spikes lasting 40s, with a 800 nM amplitude and a 15 min period. The inset shows the evolution of Ca^{2+} and cyclin B1 concentrations during the first 200 min. In the inset, the left scale (ranging from 0 to 1 μM) indicates Ca^{2+} concentration while the right scale (ranging from 0 to 2.5 μM) indicates cyclin B1 concentration. After a sufficient number of spikes, CSF decreases, which provokes a massive decrease of MPF activity and subsequent resumption of the cell cycle as shown by the regular oscillations in MPF. Results have been obtained by numerical integration of the full model for cell cycle resumption defined by eqs (3)-(8) with parameter values listed in Tables 1 and 2.*

speeds up when the level of CSF falls down. That cyclin B starts to decrease with the first fertilization-induced Ca^{2+} spikes in MII-arrested eggs has recently been demonstrated (Adjuk *et al.*, 2008). The long time delay between the first Ca^{2+} spike and CSF decrease is caused by the cascade of slow events between CaMKII activation and CSF destruction, formalized in the model by the sequential activation of hypothetical mediators S_1, S_2 and S_3. As this pathway is assumed to be cooperative, the CSF decrease is steep. It in turn induces a massive drop in the level of cyclin B, and therefore in MPF (Fig. 5, black curve). This would correspond to the extrusion of the second polar body and relief from metaphase II arrest. As CSF is now absent, cell cycle resumes normally, as indicated by the regular oscillations in MPF, each peak corresponding to a cellular division.

The model used to simulate the behaviour shown in Fig. 5 and defined by eqs(1)-(7) contains a large number of parameters. To ascribe values to these parameters, a number of facts were taken into account in the modelling approach. Parameters for CaMKII activation, listed in Table 1 are directly taken from another study where they were shown to account for the behaviour of this kinase observed *in vitro* (Dupont *et al.*, 2003). Parameters appearing in the minimal model for the cell cycle (eqs (3)-(5)), listed in Table 2, were chosen to get oscillations with a period of ~15 h in the absence of CSF and Ca^{2+}, which roughly corresponds to the time delay between successive cell divisions in mice (Kubiak *et al.*, 2008). The others, characterizing the effect of CaMKII on APC activation, were fixed (1) by the assumption that the pathway implying direct APC activation is much faster than the one leading to CSF degradation, and (2) by constraining the model to reproduce the results obtained by Toth *et al.* (2006) on the rate of activation of mouse eggs submitted to various artificial patterns of Ca^{2+} stimulation. Thus, the parameter values involved in the pathway between CaMKII activation and CSF degradation (V_{Ai}'s and V_{Di}'s in equ. (6)) must be sufficiently low to prevent egg activation in response to a single, long lasting Ca^{2+} spike (Fig. 6A). In this case, although MPF activity decreases by ~20%, CaMKII activation is not sufficient to induce CSF decrease, and thus, cell cycle does not resume. In contrast, these same parameter values

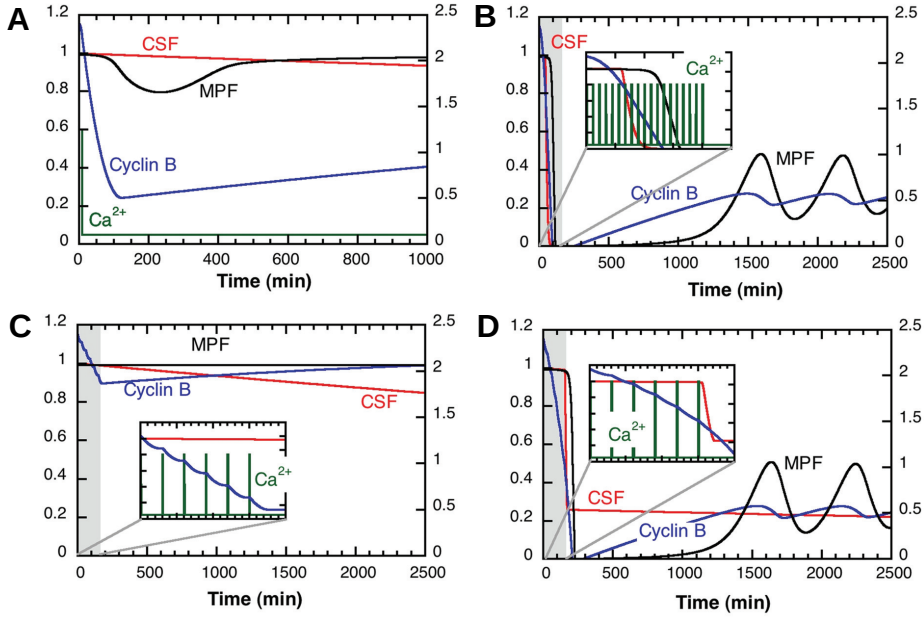

Fig. 6. Simulations of the artificial patterns of Ca^{2+} stimulation of mouse eggs described in Toth *et al.* (2006). *All panels show the evolutions of Ca^{2+} concentration, CSF activity, MPF activity (indicated on the left scale) and cyclin B1 concentration (indicated on the right scale) simulated by the model. In panels* **(B-D)**, *the grey-shaded region corresponds to the period during which the egg has been submitted to Ca^{2+} increases (of distinct characteristics depending on the panels).* **(A)** *A single Ca^{2+} peak of 600 nM amplitude and 8 min duration, corresponding to the 4HA-2min treatment of Toth* et al. *(2006), does not lead to cell cycle resumption in the model (6% of activation in the experiments).* **(B)** *5HA-19P-8min treatment, i.e. 19 Ca^{2+} peaks given at 8 min interval. Amplitude and duration equal 800nM and 1min, respectively. In the model, with this protocol, CSF is degraded and cell cycle resumes, which corresponds to the fact that egg activation is observed in the experiments in 99.6% of the cases.* **(C,D)** *An intermediate situation (6LA-30min treatment): 6 Ca^{2+} peaks with 30 min interval do not allow CSF degradation if their amplitude and duration equal 800 nM and 1 min, respectively* **(C)** *but lead to cell cycle resumption if their amplitude and duration equal 1μM and 1.5 min* **(D)**. *This can be related to the 48% rate of egg activation seen in the experiments, if it is assumed that the eggs differ by their Ca^{2+} sensitivity to the induced Ca^{2+} changes. Results have been obtained with the same equations and parameter values as in Fig. 5.*

must be large enough to allow cell cycle resumption when the egg is submitted to 19 Ca^{2+} spikes spaced out 8 min apart (Fig. 6B).

In Toth *et al.* (2006), 6 Ca^{2+} spikes, each separated by a 30 min interval were shown to activate the egg in about half the cases. The notion of 'rate of successful activation' cannot be immediately transposed in our simulations. The model indeed simulates the regulatory pathways in a single cell, and, as the model is deterministic, activation will occur, or not occur, for a given set of parameter values. A protocol leading to activation in 50% of the cases can however be interpreted as a threshold situation leading to activation in the eggs that are slightly more susceptible to process the induced Ca^{2+} changes. Thus, Fig. 6C shows that for the present choice of parameter values, 6 peaks of 0.8 μM amplitude and 1 min duration do not induce egg activation when applied every 30 min. However, with the same temporal pattern, slightly larger Ca^{2+} spikes (1 μM amplitude and 1.5 min duration) lead to cell cycle resumption in the model (Fig. 6D). This is in agreement with the fact that the 6 spikes-30 min protocol is at the border between success and failure in activation and experimentally leads to egg activation in about half the cases. In fact, with these parameter values, the model can successfully reproduce all the protocols tested by Toth *et al.* (2006). The model can thus be viewed as a satisfactory phenomenological description of the Ca^{2+}-related activatory events occurring at fertilization in mice, although the set of parameter values leading to this agreement is certainly not unique.

Computational modelling allows us to dissect signalling pathways in a manner that would not be feasible experimentally. In the model, CSF acts as the main controller as oscillations in MPF cannot resume in the presence of a high level of CSF. By contrast, a temporary decrease in MPF can be observed in the presence of CSF. Fig. 7 shows a simulation of a situation where an egg has been submitted to a single, long-lasting (8 min) Ca^{2+} spike; this leads to a significant decrease in the level of cyclin B, and thus of active MPF. However, the 8 min Ca^{2+} rise is not sufficient to induce a significant decrease in CSF activity. Thus, when Ca^{2+} is back to its basal level, APC

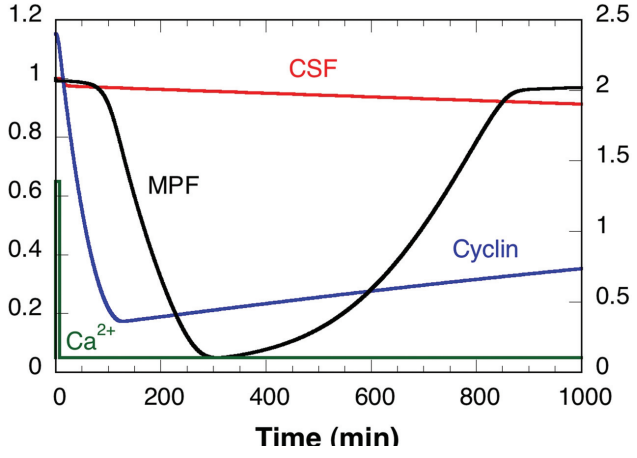

Fig. 7. Simulation of MIII arrest following an insufficient activation by Ca^{2+}. *The egg is here assumed to be stimulated by a single Ca^{2+} increase of 650 nM amplitude and lasting for 8 min. Results have been obtained with the same equations and parameter values as in Figs. 5 and 6.*

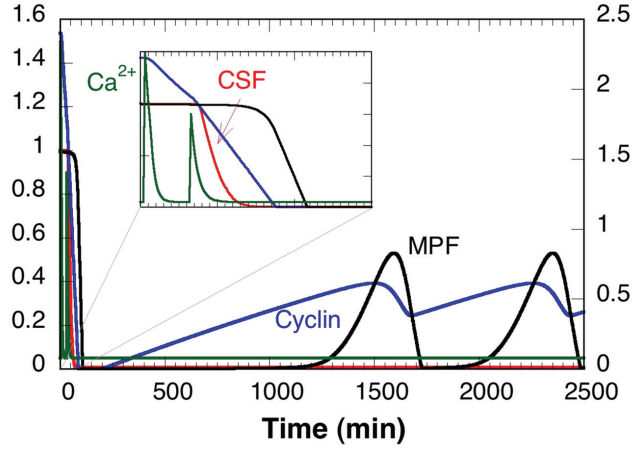

Fig. 8. Simulation of cell cycle resumption after application of two pulses of ionophores corresponding to the protocol of 'assisted oocyte activation' used by Heytens *et al.* in case of globozoospermic human patients. *Ca^{2+} increases have been fitted on Ca^{2+} data coming from this study, using two instantaneous Ca^{2+} increases followed by a bi-exponential Ca^{2+} decrease. Results have been obtained with the same equations and parameter values as in Figs. 5, 6 and 7.*

returns to an inactive state and cyclin B and MPF then reaccumulate. This behaviour, known as MIII arrest, is reminiscent of experimental observations of a transient decrease of MPF after partial activation of mouse eggs (Kubiak *et al.*, 1992; Verlhac *et al.*, 1994; Collas *et al.*, 1995).

Application of the model to in vitro *fertilization*

It is well established that the pattern of Ca^{2+} oscillations at fertilization has a direct impact on egg activation (Ozil *et al.*, 2005). This concept has long been exploited in assisted reproductive medicine in case of male infertility (Tesarik *et al.*, 1994). In particular, in couples in which intracytoplasmic sperm injection (ICSI) did not lead to successful results, fertilization rates could be improved by artificially inducing Ca^{2+} changes by treatment with Ca^{2+} ionophores, a protocol known as 'assisted oocyte activation' (AOA; Eldar-Geva *et al.*, 2003). The oocyte activating capacity is severely diminished in case of globozoospermia, a rare disorder characterized by round-headed, acrosomeless sperm cells (Schirren *et al.*, 1971; Heindryckx *et al.*, 2005). It has been shown very recently that this defect can be ascribed to anomalies in PLCζ: sperm from globozoospermic patients either displays reduced amounts of this enzyme, or contains abnormal low molecular forms of PLCζ (Yoon *et al.*, 2008; Heytens *et al.*, 2009). In agreement with this observation, human globozoospermic sperm cells are not capable of inducing long-term Ca^{2+} oscillations when injected into mouse oocytes. This kind of infertility can be overcome by combined ICSI/AOA treatment. In particular, the best rates of successful activation are obtained when eggs were submitted to two sequential Ca^{2+} pulses, as compared to only one peak.

We have used our model schematized in Fig. 2 to understand the possible physiological advantage of a two Ca^{2+} pulses protocol. Fig. 8 shows simulation results where the egg is submitted to two Ca^{2+} peaks replicating the protocol of two ionophore applications. The Ca^{2+} peak induced by the first ionophore exposure

induces a decrease in the level of cyclin B1 but does not suffice to trigger the degradation of CSF. Thus, it will not on its own allow cell cycle resumption. However, a second Ca^{2+} peak applied 30 min later (as in the ionophore treatment of Heytens *et al.*, 2008; Heindryckx *et al.*, 2005) brings about CSF degradation and cell cycle resumption. In fact, a close examination of the different variables of the model suggests that the eggs take advantage of the two peaks protocol because the pathway leading to CSF degradation (S_1 -> S_2 -> S_3) inactivates slowly. Once S_1 has been activated by the first CaMKII pulse, it remains active for some time and still activates S_2 and S_3. Thus, the time interval between the two Ca^{2+} pulses favours cell cycle resumption because the cell cycle machinery takes advantage of the on-going activation of the pathway leading to CSF degradation. For too large time intervals however, the same pathway starts to work in the opposite direction (S_3 -> S_2 -> S_1) and egg activation is not favoured anymore.

Discussion

In the present study, we have used a computational approach to look into the relationship between Ca^{2+} oscillations and cell cycle resumption at fertilization in mammals. The aim of the study was two-fold. In a first step, we wished to use a modelling approach to gain insight into the molecular mechanisms linking Ca^{2+} increases and egg activation. Although it is well established that CaMKII plays a predominant role in this respect, the detailed kinetics of CaMKII activation has never been investigated in detail. In particular, the need for repetitive Ca^{2+} spikes to activate mammalian eggs could be explained by a progressive activation of this kinase, as it occurs in other systems (De Koninck and Schulman, 1998; Swann and Yu, 2008). However, our simulations clearly show that this is not the case as CaMKII is nearly fully activated at each Ca^{2+} spike. A detailed investigation of the dynamical evolution of the kinase subunits also suggests that experimental measurements of the autonomous activity of CaMKII might be underestimated. As the summation effect of the Ca^{2+} spikes cannot be ascribed to the need for a progressive activation of CaMKII, it must rely on a pathway downstream of this kinase, which remains to be fully elucidated. We propose that experimental observations are best explained by a model where CaMKII has two effects. First, it stimulates CSF degradation by a slow pathway involving a succession of reversible steps. Second, CaMKII activates APC via a fast, but less active pathway of cyclin B1 degradation. For an appropriate set of parameter values, the model then allows to reproduce experimental observations related to egg activation in response to imposed Ca^{2+} pulses. As a consequence of this dual activation pathway, the decrease in cyclin B concentration can either precede or follow the drop in CSF in the model. The versatility in the precise timing of decreases of these two components is open to be further assessed experimentally. Moreover, in the model, the rate of cyclin B decrease due to the CSF-independent pathway is highly sensitive to the frequency of Ca^{2+} oscillations. In contrast, as CSF acts as an all-or-none brake on the cell cycle, its decrease provokes a sudden and rapid decrease in the level of cyclin B, which is then independent of the frequency of the Ca^{2+} spikes. The time needed to decrease CSF depends on the Ca^{2+} pattern, but not the slope of the decrease in cyclin B once CSF has dropped. Thus, it may be interesting to relate in experiments the rate of cyclin B decrease to the frequency of Ca^{2+} oscillations to assess the existence of a CSF-independent pathway of egg activation.

In a second step, we propose that the model can be used to test the efficacy of artificial protocols of egg activation in human assisted reproductive medicine. Although these model predictions are related to data obtained in mice, it accounts for the observation that two pulses of ionophore given at 30 min interval maximises the rate of success of intracytoplasmic sperm injection in case of male infertility due to globozoospermia in humans. In fact, the model suggests that the time interval between the two Ca^{2+} peaks allows for the accumulation of the activity leading to CSF degradation. The existence of an optimal time interval between two peaks of stimulation is known to occur in hormonal signalling systems, where the physiological response is often optimized at intermediate frequencies of stimulation (Li and Goldbeter, 1989).

The model presented in this study involves many unknowns, both at the level of the signalling pathway itself and concerning the choice of parameter values. It must be viewed as a useful, but empirical approach to the process of egg activation. The most speculative part of the model is the direct activation of APC by CaMKII. As emphasized above, this regulation must be viewed as any possible fast pathway of APC activation, independent from CSF degradation that can occur as soon as Ca^{2+} starts to spike (Adjuk *et al.*, 2008). It may be related to the c-Mos/MAPK pathway as suggested in Madgwick and Jones (2007). This pathway allows to account for the partial and reversible cyclin B1 degradation observed at each Ca^{2+} spike. It could be argued that each Ca^{2+} spike instead provokes the degradation of a small amount of CSF. However, the latter view does not hold with a possible evolution to MIII-arrested state as CSF destruction is irreversible. The exact molecular targets involved in this pathway could be particularly difficult to uncover, as it is by nature transient. However, these may be similar to those linking Ca^{2+} increase and metaphase to anaphase transition in the mitotic cell cycle (Ciapa *et al.*, 1994).

At the level of CaMKII activation, the way in which phosphatases are included in the model is also somewhat arbitrary. Data about this activity in the mature oocyte are indeed limited, although one can expect them to have a significant impact on egg activation. PP1, PP2A and PP2B may be involved in reversing CaMKII activation (Ducibella and Fissore, 2008). Calmodulin concentration is another potentially important parameter that has not been determined. Estimates for calmodulin concentrations in cells fall in the range 1 to 5 μM (Persechini and Stemmer, 2002). Here, we have taken 1 μM to take into account the possible spatial localization of CaMKII activation, as well as the fact that there are many other targets for CaM binding. Given that the K_D of Ca^{2+} for CaM is 1 μM, it means that CaM could be limiting for CaMKII activation when the increase of Ca^{2+} is especially massive, as during the fertilization wave in some protocols of artificial egg activation. To assess this possibility, it would be interesting to manipulate the level of CaM in the fertilized egg to see if it can affect the rate of egg activation.

Ca^{2+} oscillations at fertilization have other functions than promoting exit from meiosis (Ducibella and Fissore, 2008; Kubiak *et al.*, 2008). In particular, CaMKII contributes to the membrane block to polyspermy, via a pathway involving actin regulation (Gardner *et al.*, 2007). Ca^{2+}-dependent recruitments of specific

maternal mRNAs and translationally-regulated changes in protein expression have also been reported. These phenomena most probably involve other Ca^{2+}-sensitive kinases and phosphatases. Understanding how Ca^{2+} can specifically activate this variety of processes represents another challenge both for experimentalists and modellers.

Acknowledgements

G.D. acknowledges support from the Fonds de la Recherche Scientifique Médicale (grant #3.4636.04), the European Union through the Network of Excellence BioSim (Contract #LSHB-CT-2004-005137) and the Belgian Program on Interuniversity Attraction Poles, initiated by the Belgian Federal Science Policy Office, project #P6/22 (BIOMAGNET). This work was supported by grants from the Found for Scientific Research Flanders and the Interuniversity Attraction Poles Program (Belgian Science Policy, project P6/3 to L.L.) GD is Maître de Recherche at the Belgian Fonds National de la Recherche Scientifique. EH is supported by the Special Research Foundation (BOF) of Ghent University.

References

ADJUK, A., CIEMERYCH, M., NIXON, V., SWANN, K. and MALESZEWSKI, M. (2008). Fertilization differently affects the levels of cyclin B1 and M-phase promoting factor activity in maturing and metaphase II mouse oocytes. *Reproduction* 136: 741-752.

BERRIDGE, M.J. (2008). Inositol trisphosphate and calcium signalling mechanisms. *Biochim. Biophys. Acta* (In press).

BRAUN, A. and SCHULMAN, H. (1995). The multifunctional calcium/calmodulin-dependent protein kinase: from form to function. *Annu. Rev. Physiol.* 57: 417-445.

CIAPA, B., PESANDO, D., WILDING, M. and WHITAKER, M. (1994). Cell-cycle calcium transients driven by cyclic changes in inositol trisphosphate levels. *Nature* 368: 875-878.

COLLAS, P., CHANG, T., LONG C. and ROBL, J.M. (1995). Inactivation of histone H1 kinase by Ca^{2+} in rabbit oocytes. *Mol. Reprod. Dev.* 40: 253-258.

CSIKASZ-NAGY, A., BATTOGTOKH, D., CHEN, K.C., NOVAK, B. and TYSON, J. (2006). Analysis of a generic model of eukaryotic cell-cycle regulation. *Biophys. J.* 90: 4361-4369.

DE PITTA, M., VOLMAN, V., LEVINE, H., PIOGGIA, G., DE ROSSI, D. and BEN-JACOB, E. (2008). Coexistence of amplitude and frequency modulations in intracellular calcium dynamics. *Phys. Rev. E* 77: 030903-1-4.

DE KONINCK, P. and SCHULMAN, H. (1998). Sensitivity of CaM kinase II to the frequency of Ca^{2+} oscillations. *Science* 279: 227-230.

DUCIBELLA, T., SCHULTZ, R. and OZIL, J.-P. (2006). Role of calcium signals in early development. *Sem. Cell & Dev. Biol.* 17: 324-332.

DUCIBELLA, T. and FISSORE, R. (2008). The roles of Ca^{2}, downstream protein kinases, and oscillatory signaling in regulating fertilization and the activation of development. *Dev. Biol.* 315: 257-279.

DUPONT, G. (1998). Link between fertilization-induced Ca^{2+} oscillations and relief from metaphase II arrest in mammalian eggs: a model based on calmodulin-dependent kinase II activation. *Biophys. Chem.* 72: 153-167.

DUPONT, G., HOUART, G. and DE KONINCK, P. (2003). Sensitivity of CaM kinase II to the frequency of Ca^{2+} oscillations: a simple model. *Cell Calcium* 34: 485-497.

DUPONT, G. and DUMOLLARD, R. (2004). Simulations of calcium waves in ascidian eggs: insights into the origin of the pacemaker sites and the possible nature of the sperm factor. *J. Cell Science* 117: 4313-4323.

DUPONT, G., COMBETTES, L. and LEYBAERT, L. (2007). Calcium dynamics: spatio-temporal organization from the subcellular to the organ level. *Int. Rev. Cytology* 261: 193-245.

ELDAR-GEVA, T., BROOKS, B., MARGALIOTH, E., ZYLBER-HARAN, E., GAL, M. and SILBER, S. (2003). Successful pregnancy and delivery after calcium ionophore oocyte activation in a normozoospermic patient with previous repeated failed fertilization after intracytoplasmic sperm injection. *Fertil Steril.* 79 Suppl 3: 1656-1658.

FALL, C., WAGNER, J., LOEW, L. and NUCCITELLI, R. (2004). Cortically restricted production of IP_3 leads to propagation of the fertilization Ca^{2+} wave along the cell surface in a model of the *Xenopus* egg. *J. Theor. Biol.* 231: 487-496.

GARDNER, A., KNOTT, J., JONES, K. and EVANS J. (2007). CaMKII can participate in but is not sufficient for the establishment of the membrane block to polyspermy in mouse eggs. *J. Cell. Physiol.* 212: 275-80.

GOLDBETER, A. (1991). A minimal cascade model for the mitotic oscillator involving cyclin and cdc2 kinase. *Proc. Natl. Acad. Sci. USA* 88: 9107-9111.

HANSEN, D., TUNG, J. and JACKSON, P. (2006). CamKII and Polo-like kinase 1 sequentially phosphorylate the cytostatic factor Emi2/Xerp1 to trigger its destruction and meiotic exit. *Proc. Natl. Acad. Sci. USA* 103: 608-613.

HEINDRYCKX, B., VAN DER ELST, J., DE SUTTER, P. and DHONT, M. (2005). Treatment option for sperm- or oocyte-related fertilization failure: assisted oocyte activation following diagnostic heterologous ICSI. *Hum. Reprod.* 20: 2237-2241.

HEYTENS, E. SOLEIMANI, R., LIERMAN, S., DE MEESTER, S., GERRIS, J., DHONT, M., VAN DER ELST, J. and DE SUTTER, P. (2008). Effect of ionomycin on oocyte activation and embryo development in mouse. *Reprod. Biomed. Online* 17: 764-71.

HEYTENS, E., PARRINGTON, J., COWARD, K., LAMBRECHT, S., YOUNG, C., SOLEIMANI, R., CUVELIER, C., GERRIS, J., DHONT, M., DEFORCE, D., LEYBAERT, L. and DE SUTTER, P. (2009). Reduced amounts and abnormal forms of phospholipase C zeta in spermatozoa from infertile men. *Human Reprod.* 24: 2417-2428 (doi: 10.1093/humrep/dep207).

JONES, K. (2005). Mammalian egg activation: from Ca^{2+} spiking to cell cycle progression. *Reproduction* 130: 813-823.

KNOTT, J., GARDNER, A., MADGWICK, S., JONES, K., WILLIAMS, C. and SCHULTZ, R. (2006). Calmodulin-dependent protein kinase II triggers mouse egg activation and embryo development in the absence of Ca^{2+} oscillations. *Dev. Biol.* 296: 388-395.

KUBIAK, J., WEBER, M., GERAUD, G. and MARO, B. (1992). Cell cycle modification during the transition between meiotic M-phases in mouse oocytes. *J. Cell Science* 102: 457-467.

KUBIAK, J., CIEMERYCH, M., HUPALOWSKA, A., SIKORA-POLACZEK, M. and POLANSKI, Z. (2008). On the transition from the meiotic to mitotic cell cycle during early mouse development. *Int. J. Dev. Biol.* 52: 201-217.

LARSEN, A., OLSEN, L., KUMMER, U. (2004). On the encoding and decoding of calcium signals in hepatocytes. *Biophys. Chem.* 107: 83-99.

LI, Y.X. and GOLDBETER, A. (1989). Frequency specificity in intercellular communication. Influence of patterns of periodic signaling on target cell responsiveness. *Biophys. J.* 55: 125-145.

MADGWICK, S., LEVASSEUR, M. and JONES, K. (2005). Calmodulin-dependent protein kinase II, and not protein kinase C, is sufficient for triggering cell-cycle resumption in mammalian eggs. *J. Cell Science* 118: 3849-3859.

MADGWICK, S., HANSEN, D., LEVASSEUR, M., JACKSON, P. and JONES, K. (2006). Mouse Emi2 is required to enter meiosis II by restablishing cyclin B1 during interkinesis. *J. Cell Biol.* 174: 791-801.

MADGWICK, S. and JONES K. (2007). How eggs arrest at metaphase II: MPF stabilisation plus APC/C inhibition equals cytostatic factor. *Cell Division* 2:4 doi:10.1186/1747-1028-2-4.

MALCUIT, C., KUROKAWA, M. and FISSORE, R. (2006). Calcium oscillations and mammalian egg activation. *J. Cell. Phyisol.* 206: 565-573.

MARKOULAKI, S., MATSON, S. and DUCIBELLA, T. (2004). Fertilization stimulates long-lasting oscillations of CaMKII activity in mouse eggs. *Dev. Biol.* 272: 15-25.

MARKOULAKI, S., KUROKAWA, M., YOON, S.-Y., MATSON, S., DUCIBELLA, T. and FISSORE, R. (2007). Comparison of Ca^{2+} and CaMKII responses in IVF and ICSI in the mouse. *Mol. Hum. Reprod.* 13: 265-272.

MASUI, Y. and MARKET, C. (1971). Cytoplasmic control of nuclear behavior during meiotic maturation of frog oocytes. *J. Exp. Zool.* 117: 129-145.

MARKOULAKI, S., MATSON, S. and DUCIBELLA, T. (2004). Fertilization stimulates long-lasting oscillations of CaMKII activity in mouse eggs. *Dev. Biol.* 272: 15-25.

MORRIS, E.P. and TOROK, K. (2001). Oligomeric structure of α-calmodulin-

dependent protein kinase II. *J. Mol. Biol.* 308: 1-8.

MUKHERJI, S. and SODERLING, T. (1994). Regulation of Ca^{2+}/calmodulin-dependent protein kinase II by inter- and intrasubunit-catalyzed autophosphorylation. *J. Biol. Chem.* 269: 13744-13747.

NURSE, P. (2002). Nobel Lecture. Cyclin dependent kinases and cell cycle control. *Biosci. Rep.* 22: 487-499.

OZIL, J.-P. (1998). Role of calcium oscillations in mammalian egg activation: experimental approach. *Biophys. Chem.* 72: 141-152.

OZIL, J.-P., MARKOULAKI, S., TOTH, S., MATSON, S., BANREZES, B., KNOTT, J., SCHULTZ, R., HUNEAU, D. and DUCIBELLA, T. (2005). Egg activation events are regulated by the duration of a sustained $[Ca^{2+}]_{cyt}$ signal in the mouse. *Dev. Biol.* 282: 39-54.

PERSECHINI, A. and STEMMER, P. (2002). Calmodulin is a limiting factor in the cells. *Trends Cardiovasc. Med.* 12: 32-37.

RAUH, N.R., SCHMIDT, A., BORMANN, J., NIGG, E.A. and MAYER, T.U. (2005). Calcium triggers exit from meiosis II by targeting the APC/C inhibitor XErp1 for degradation. *Nature* 437: 1048-1052.

RUNFT, L., JAFFE, L. and MEHLMANN, L. (2002). Egg activation at fertilization: where it all begins. *Dev. Biol.* 245: 237-254.

SAGATA, N. and WATANABE, G. (1989). The *c-mos* proto-oncogene product is a cytostatic factor responsible for meiotic arrest in vertebrate eggs. *Nature* 342: 512-518.

SAUNDERS, C., LARMAN, M., PARRINGTON, J., COX, L., ROYSE, J., BLAYNEY, L., SWANN, K. and LAI, F. (2002). PLCζ: a sperm-specific trigger of Ca^{2+} oscillations in eggs and embryo development. *Development* 129: 3533-3544.

SCHIRREN, C., HOLSTEIN, A. and SCHIRREN, C. (1971). Uber die Morphogenese rundkopFiger Spermatozoen des Menschen. *Andrologie* 3: 117-125.

SCHMIDT, A., DUNCAN, P., RAUH, N., SAUER, G., FRY, A., NIGG, E. and MAYER, T. (2005). *Xenopus* polo-like kinase Plx1 regulates Xerp1, a novel inhibitor of APC/C activity. *Genes Dev.* 19: 502-513.

SNEYD, J., KEIZER, J. and SANDERSON, M. (1995). Mechanisms of calcium oscillations and waves: A quantitative analysis. *FASEB J.* 9: 1463-1472.

STRICKER, S. (1999). Comparative biology of calcium signaling during fertilization and egg activation in animals. *Dev. Biol.* 211: 157-176.

SWANN, K. and YU, Y. (2008) The dynamics of calcium oscillations that activate mammalian eggs. *Int. J. Dev. Biol.* 52: 571-584.

TESARIK, J., SOUSA, M. and TESTART, J. (1994). Human oocyte activation after intracytoplasmic sperm injection. *Hum. Reprod.* 9: 511-518.

TOTH, S., HUNEAU, D., BANREZES, B. and OZIL, J.-P. (2006). Egg activation is the result of calcium signal summation in the mouse. *Reproduction* 131: 27-34.

VERLHAC, M., KUBIAK, J., CLARKE, H. and MARO, B. (1994). Microtubule and chromatin behavior follow MAP kinase activity but not MPF activity during meiosis in mouse eggs. *Dev.* 120: 1017-1025.

WATANABE, N., HUNT, T., IKAWA, Y. and SAGATA, N. (1991). Independent inactivation of MPF and cytostatic factor (Mos) upon fertilization of *Xenopus* eggs. *Nature* 352: 247-248.

YOON, S., JELLERETTE, T., SALICIONI, A., LEE, H., YOO, M. *et al.* (2008). Human sperm devoid of PLC zeta 1 fail to induce Ca^{2+} release and are unable to initiate the first step of embryo development. *J. Clin. Invest.* 118: 3671-3681.